Available online at www.sciencedirect.com
SCIENCE DIRECT®
Polymer 45 (2004) 3473–3480
polymer
www.elsevier.com/locate/polymer

A study of the versatile micropatterns of diblock copolymer micelles: the effect of copolymer concentration, substrate, film thickness and micelles morphology

Yannie Chan, Yongli Mi*

Department of Chemical Engineering, The Hong Kong University of Science and Technology, Clear Water Bay, Kowloon, Hong Kong

Received 17 December 2003; received in revised form 17 February 2004; accepted 17 February 2004

Abstract

We report the novel use of polystyrene-*block*-poly(acrylic acid) (PS-*b*-PAA) diblock copolymer micelles as the nano-building blocks in fabricating orderly aligned three-dimensional micropatterns with high regularity through a one-step evaporation-induced cracking process. Crack patterns of square, rectangular, stripe-like and mesh-like structures in micron scale were obtained. The effect of the concentration of diblock copolymer, the properties of the substrates, the thickness of the drying layer, and the morphology of the micelles on the regularity of the crack patterns was studied. By regulating the above factors, we achieved micropatterns of various structures. We further developed a cheap, fast, and simple method for fabricating micromolded structures using the crack patterns as templates.

Keywords: Diblock copolymer micelles; Micropatterns

1. Introduction

Crack formation upon drying or cooling is a common phenomenon observed in everyday life. Surfaces of paint, mud [1], flour, and the latex solution [2], among others, can crack when left evaporating under ambient condition. Natural occurrence of crack patterns can also be noticed from the preserved geological ancient crack patterns [3], columnar joints [4], or the huge ice-cracks in the arctics [5]. A considerable amount of studies have been carried out to investigate the cracking phenomena, both experimentally [6,7] and theoretically [8,9]. Recently, the colloidal system of Al_2O_3 particles in water has been used to study shrinkage-crack patterns [10]. Crack patterns are formed when multiple cracks are developed and interconnected. Cracks appear as a result of material contraction during cooling or drying, as changes in humidity and/or temperature lead to a build-up of stress in the material. Once the accumulated stress exceeds the local tensile strength of the material, it has to be released. As a result, cracks occur in the dried material. The stress concentrates at the crack tips and results in a forward propagation of cracks, which are initiated perpendicularly to the drying front and penetrate inward to the interior region at a constant speed, leading to unidirectional primary cracks. Then, the stress on the parallel cracks induces secondary crack nucleation that propagates perpendicularly to the primary cracks to form a tiling pattern [10]. Among the various studies and investigations on the cracking phenomenon, there is not a single report on the control of the crack pattern to form a well-organized and regularly aligned micropattern with potential applications.

Numerous studies of diblock copolymer micelles and the micelle morphology have been reported in the past decade [11–16]. In this paper, we report the formation of diblock copolymer micropatterns based on the crack mechanisms described above. We achieved crack patterns with controlled regularity, as shown in Fig. 1. A number of orderly patterned structures like squares, rectangles, stripes-like and mesh-like structures were obtained. This study reveals the crack pattern formation by evaporation-induced self-assembly of diblock copolymer micelles. We then used the crack patterns as templates for molding useful microstrutures. Compared to existing microfabrication technologies, our method is simple and less time-consuming.

* Corresponding author. Tel.: +852-2358-7127; fax: +852-2358-0054.
E-mail address: keymix@ust.hk (Y. Mi).

0032-3861/$ - see front matter © 2004 Elsevier Ltd. All rights reserved.
doi:10.1016/j.polymer.2004.02.033

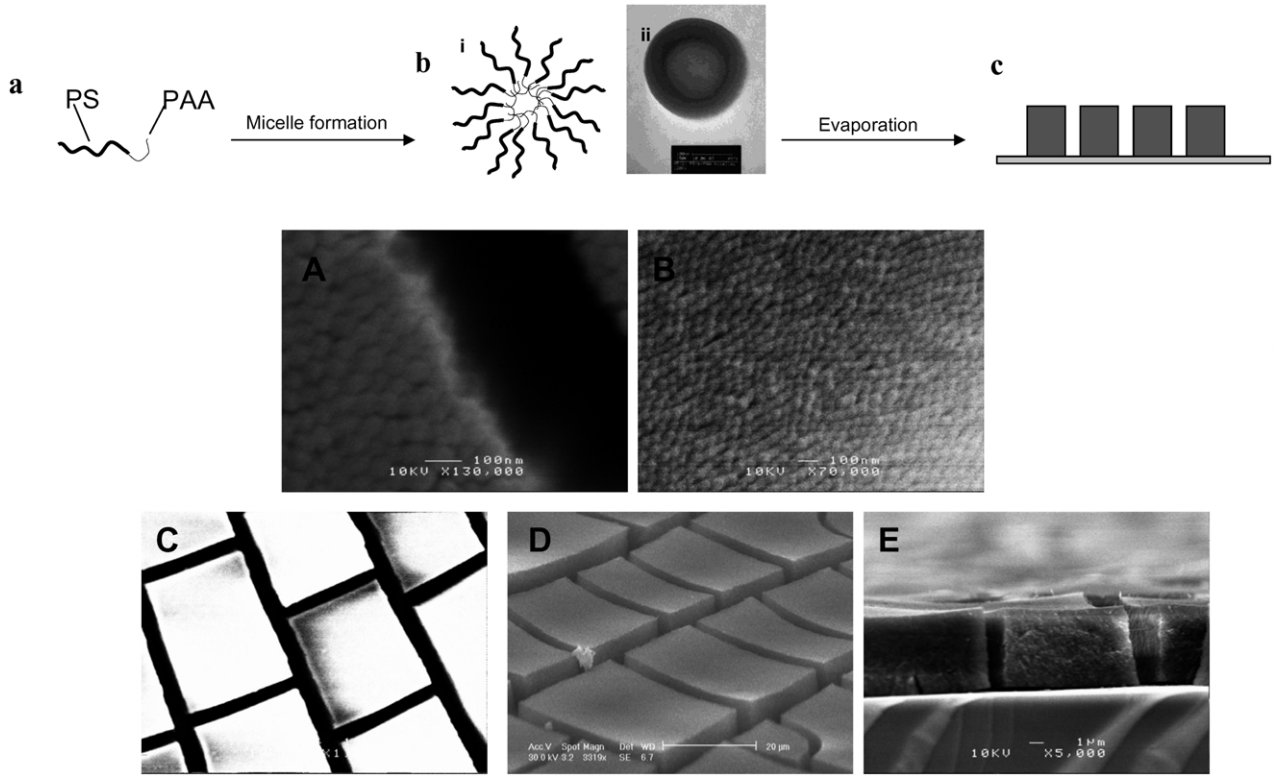

Fig. 1. The schematic diagram showing a stepwise self-assembly of PS-*b*-PAA diblock copolymer (a) into micelle (b-i), and the evaporation-induced crack micropattern formation (c). The TEM micrograph of a single vesicular micelle (b-ii), and the diameter of the single micelles is about 50 nm. The SEM micrographs of aggregated micelles (A, B). The top-view (C), side-view (D), and cross-section (E) of the SEM micrographs of the three-dimensional micropattern.

2. Experimental section

2.1. Preparation of diblock copolymer micelles

The diblock copolymer, polystyrene-*block*-poly(acrylic acid) (PS-*b*-PAA) (P1541-SAA) was purchased from Polymer Source, Inc., Que., Canada. The material is amphiphilic, with a hydrophobic PS block of M_n: 66,500 and a hydrophilic PAA block of M_n: 4500. The molecular weight distribution of the sample is narrow with an M_w/M_n of 1.08. This intrinsic property allows the self-assembly of the diblock copolymer into a spherical micellar structure. To prepare a diblock copolymer solution, the PS-*b*-PAA was dissolved in tetrahydrofuran (THF), with the concentration range of 8–10 mg/ml. Nanopure deionized water was added drop-wise at the rate of 1 drop per 10 s with mild stirring till the final concentration of 0.09 v/v was reached. The morphology and diameter of the micelles were determined by transmission electron microscopy (TEM Jeol 100CXII) and scanning electron microscopy (SEM Jeol 6300F) and are illustrated in Fig. 1(B) (ii) and Fig. 1(A) and (B), respectively.

2.2. Formation of the micropattern

The N-type silicon wafer was chosen as the substrate for the micropattern formation. It was fractionated into smaller sizes and washed with 2-propanol first and then with water. A certain volume of micelle solution was pipetted onto the substrate and was kept drying inside a fume hood with a dust free environment and at a constant airflow rate in the ambient condition.

The crack micropattern obtained upon drying was observed by the optical microscopy (Olympus BX-41, Japan, equipped with the Leica DC100 CCD color camera) and by SEM.

3. Result and discussion

3.1. Micropatterns

A number of orderly aligned three-dimensional crack patterns in micron scale were obtained by evaporation of the diblock copolymer micelles solution. Referring to Figs. 1 and 2, different structures, such as the cubic blocks (Figs. 1(D), (E) and 2(A)), the rectangular blocks (Fig. 2(B) and (C)) and the stripe-like structures (Fig. 2(D)), were observed. Distinct and explicit edges and right-angled corners were observed through SEM. The block-to-block distance, the width of crack channels, was estimated from the cross-sectional view of SEM in Fig. 1(E) to be about

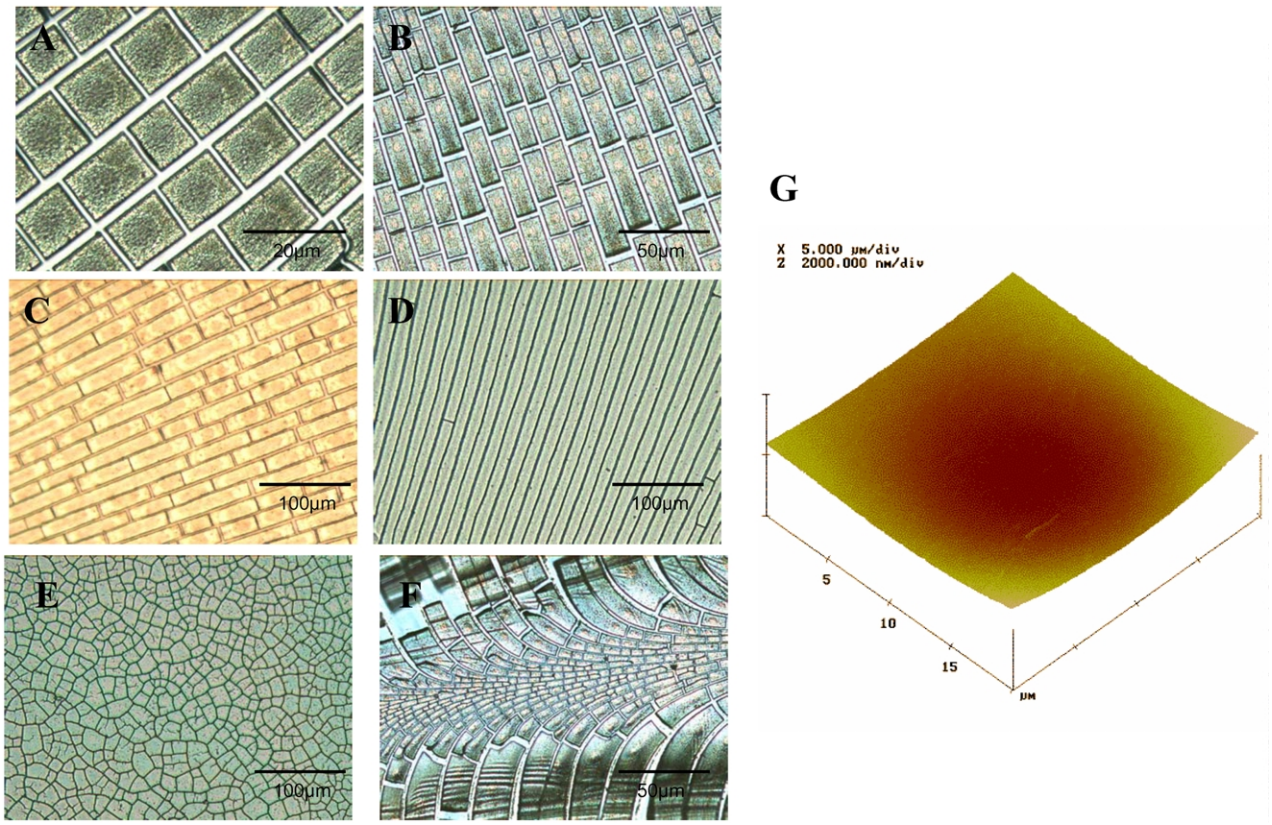

Fig. 2. The optical micrographs showing the various crack patterns of diblock copolymer micelle solution: square (A), rectangle (B), longer rectangle (C), stripe-like (D), mesh-like (E), and structure with special configuration (F). AFM reveals the slightly concave topology at the center of the block surface (G).

1 μm. A surface profiler system (Alpha-Step 2000) was also used to measure the dimensions and distances of the blocks. It was found that the width and the height of the blocks were about 10 μm, whereas the length of the blocks varies. The blocks are patterned in even spacing. Corresponding to the theoretical prediction [1,6–8], the dimension of the crack blocks is about the same as the thickness of the dried layer. In order to study the crack pattern formation in detail, the evaporation process was video-recorded by a digital video camera (Sony 3CCD color video camera). Cracks were initiated at the solution boundary and were propagated inwards with a constant speed. The unidirectional cracks resulted in an array of uniformly spaced microchannels (cf. Fig. 2(B)). Secondary cracks could also be nucleated by further drying and they penetrated perpendicularly into the pre-existing stripe-like pattern, giving rise to the orderly aligned quadrate micropatterns. When both primary and secondary cracking are not linear, non-directional propagation of cracks may result in irregular patterns or polygonal patterns (cf. Fig. 2(E)). Cracks may also nucleate from the inhomogeneities on the substrate or in the micelle solution. Such crack patterns would have less regular conformation and orientation [9]. In this case, bifurcations or branching could be observed. A collection of quadrate patterns showing a trend of morphology transition from squares, rectangles and stripe-like structures, by controlling the diblock copolymer concentrations in THF, is demonstrated in Fig. 2. The optimum range of concentration for the square pattern (Fig. 2(A)) was found to be 9.5–10 mg/ml, for the rectangular pattern (Fig. 2(B)) 9.2–9.5 mg/ml, for the longer rectangles (Fig. 2(C)) 8.5–9.2 mg/ml, and for the stripe-like structures (Fig. 2(D)) 8.0–8.5 mg/ml. Atomic force microscopy (AFM) study of the block surface revealed a slightly concave topology as shown in Fig. 2(G). The depth of the concavity is about 0.1 μm. In addition to the quadrate micropatterns, stripe-like (Fig. 2(D)), mesh-like (Fig. 2(E)), and intermediate transient structures (Fig. 2(F)) were also achieved by adjusting the parameters in preparing the micelles solution such as the polymer concentration and the solvent ratio.

3.2. Effect of the substrate

Substrates of different materials and surface flatness have been used to investigate the crack pattern formation. Three different surfaces were studied, namely: glass surface, silicon wafer sputtered with a gold layer of 100 micron (Sputter Coater for Gold—Denton Vacuum DESKII), and silicon wafer sputtered first with 100 nm of titanium and then 400 nm of gold (Thin Film Sputtering System—Denton Vacuum Discovery 18). The purpose of using titanium coating was to improve the surface adhesion of gold particles and the surface flatness. The surface colors of the two-coated wafers are different. The gold sputtered

silicon wafer has a shiny copper appearance while the titanium–gold sputtered one is of a bright golden color. Crack micropattern formation on the three different substrates were illustrated in Fig. 3. Fig. 3(A) and (B) shows the micropatterns formed on the glass substrate; Fig. 3(C) and (D) show the micropatterns formed on the gold sputterd silicon wafer; and Fig. 3(E) and (F) shows the crack pattern formed on the surface of the titanium–gold bilayer on silicon wafer. It is seen from Fig. 3 that the glass surface and the gold sputterd silicon wafer surface resemble each other in the shape and regularity of crack micropattern, which is similar to the results obtained on the silicon wafers as shown in Figs. 1 and 2. The surface of the titanium–gold bilayer on silicon wafer resulted in quite irregular and polygonal patterns, as shown in Fig. 3(E) and (F). Repeated experiments revealed that the crack micropattern formation on the titanium–gold bilayer was uncontrollable and the crack pattern was unpredictable. This could be attributed to the extreme smoothness of the titanium–gold layer surface that causes slipping at the bottom of the film during the evaporation process. The block sizes would, therefore, be larger, which corresponds to a previous study by Groisman and Kaplan that the size of crack cells increased in the case of a 'slippery bottom' [6]. Likewise, the crack blocks on the gold surface were smaller than those on the titanium–gold surface, but larger than those on the glass substrate. In addition, crack blocks on the glass surface were more often to be square in shape, while those on the two gold surfaces were generally rectangular. This may also be attributed to the 'slipping bottom' effect whereby the smoother gold surface can grant more mobility, so that the crack pattern would be in rectangle or longer rectangle.

3.3. Effect of the film thickness

Previous studies revealed that both the film thickness and the diffusion profiles play an important role in the stability of crack formation [1,6]. Groisman and Kaplan carried out experiments on drying coffee–water mixture and discovered that the size or the width of the cracked pattern was nearly proportional to the thickness of the drying layer. The effect of varying the film thickness on the crack pattern formation has also been investigated. It was found that a decrease in film thickness resulted in a transition of structures from straight cracks with right-angled junctions to wavy cracks with Y-sharped (120°) junctions [6]. Similar

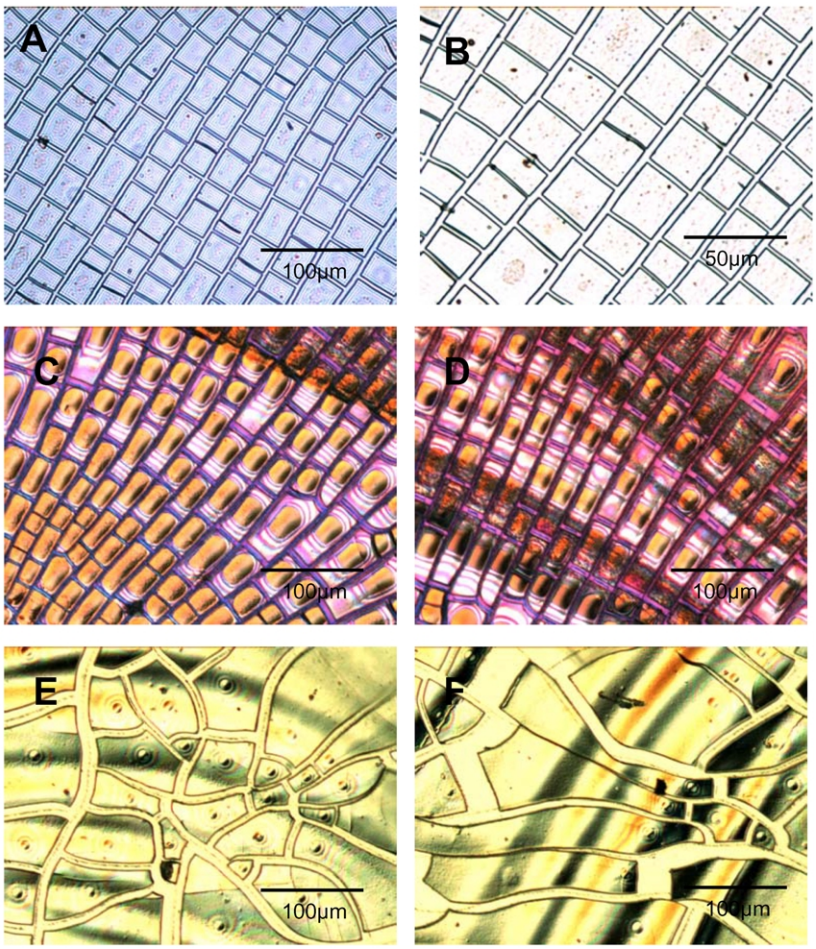

Fig. 3. Effect of substrates on micropattern structures. Micropatterns formed by evaporation on different substrates: glass surface (A, B); gold sputtered silicon wafer (C, D); gold sputtered on titanium coated silicon wafer (E, F).

results were obtained in our experiment using diblock copolymer micelle solution for the crack pattern formation. Droplet of the diblock copolymer solution of a concentration of 10 mg/ml PS-*b*-PAA in THF with 0.09 v/v of nano pure water was pipetted onto 5×5 mm^2 silicon wafer. Different drop volumes—2, 3, 5, 10, and 15 μl/drop—were cast on the substrates. The different volume gave the film different thicknesses after drying. Fig. 4 shows the different crack patterns resulting from the increasing thickness of the drying films. Irregular mesh-like crack patterns were observed in the 2 μl/drop sample as shown in Fig. 4(A). Y-shaped patterns were observed in the 3 μl/drop sample as shown in Fig. 4(B). Fig. 4(C) shows that, for the 5 μl/drop sample, there is more pronounced regularity. For the 10 μl/drop sample, Fig. 4(D) shows the majority of the crack patterns are regularly shaped squares. For the 15 μl/drop sample, Fig. 4(E) shows an array of squares with even higher regularity and orderness. No Y-shape cracks or polygonal structures were observed. In addition, the pattern size of the 15 μl/drop sample was much larger than the previous samples. This observation concluded that an increase in the film thickness of the diblock copolymer solution facilitates an increase in the orderliness of the micropattern. Repeated experiments were performed using silicon wafer substrates 20×20 mm^2 in size and with even higher drop volume. Fig. 4(F) and (G) show the patterns formed on the 60 μl/drop and the 80 μl/drop samples, respectively. It is clear that the 60 μl/drop sample gives a pattern that is a mixture of squares and rectangles, while the 80 μl/drop sample presents a pattern of orderly aligned rectangles. Tiling blocks were separated by straight, parallel and continuous microchannels, meeting at right-angled junctions.

The orderliness of crack pattern decreases with the increase in film thickness, a phenomenon that can be correlated with the diffusion profile of the drying system. Crack formation is crucially determined by the changes in humidity and temperature distribution of the evaporating system [8]. A larger volume of micelles solution implies a thicker evaporating film and a sharper drying front. Therefore, a steeper humidity and temperature gradient along the surface will be induced, which enables a rapid build-up of stress within the system. To relieve the instantaneously accumulated stress, cracks start to propagate along the receding direction of the drying front. For the thicker drying layers, the crack stability enables a stronger

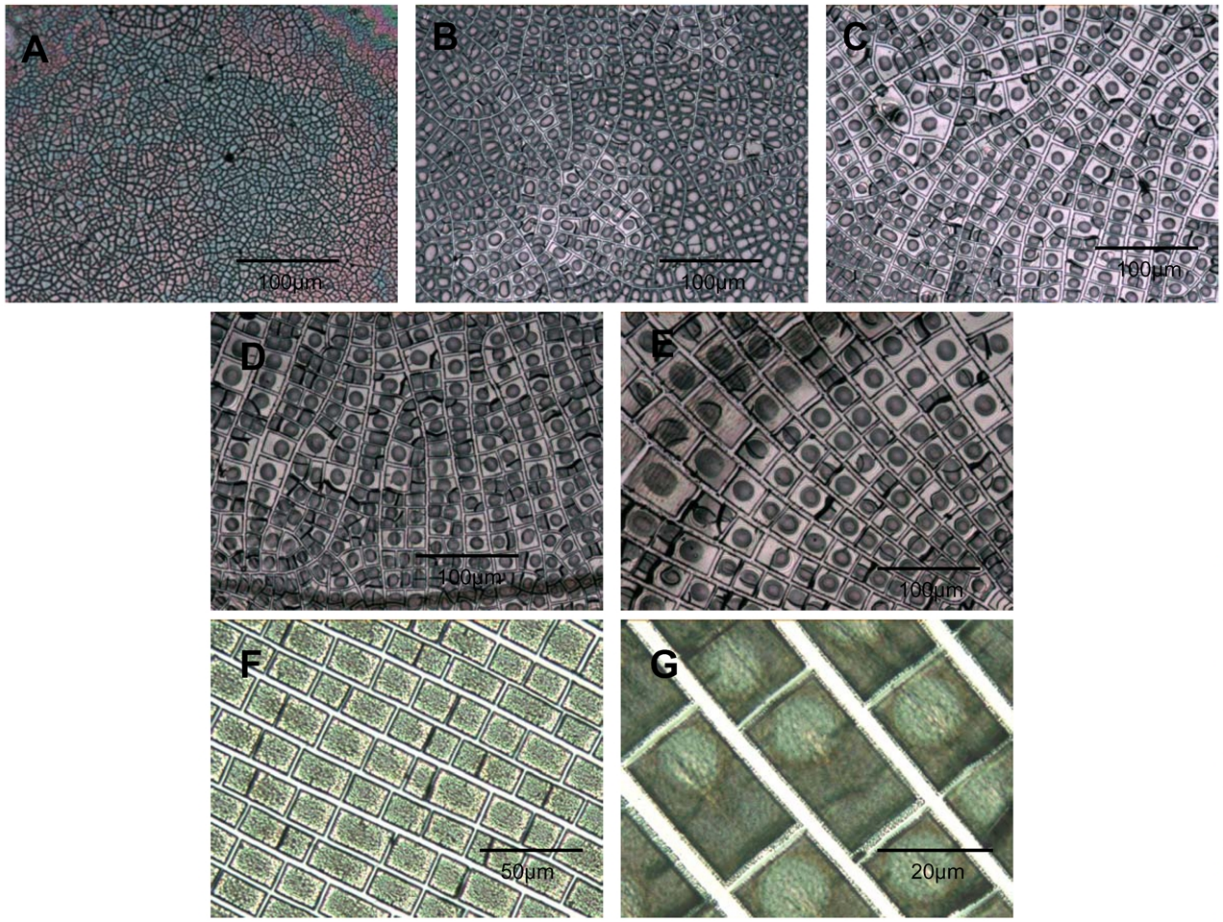

Fig. 4. Effect of film thickness on micropatterns. Micropatterns formed from increasing the film thickness by dropping 2, 3, 5, 10 and 15 μl of micelle solution onto 5×5 mm^2 silicon wafer substrates, respectively (A–E). Micropatterns formed by evaporating 60 and 80 μl of micelle solution at 20×20 mm^2 silicon wafer, respectively (F, G).

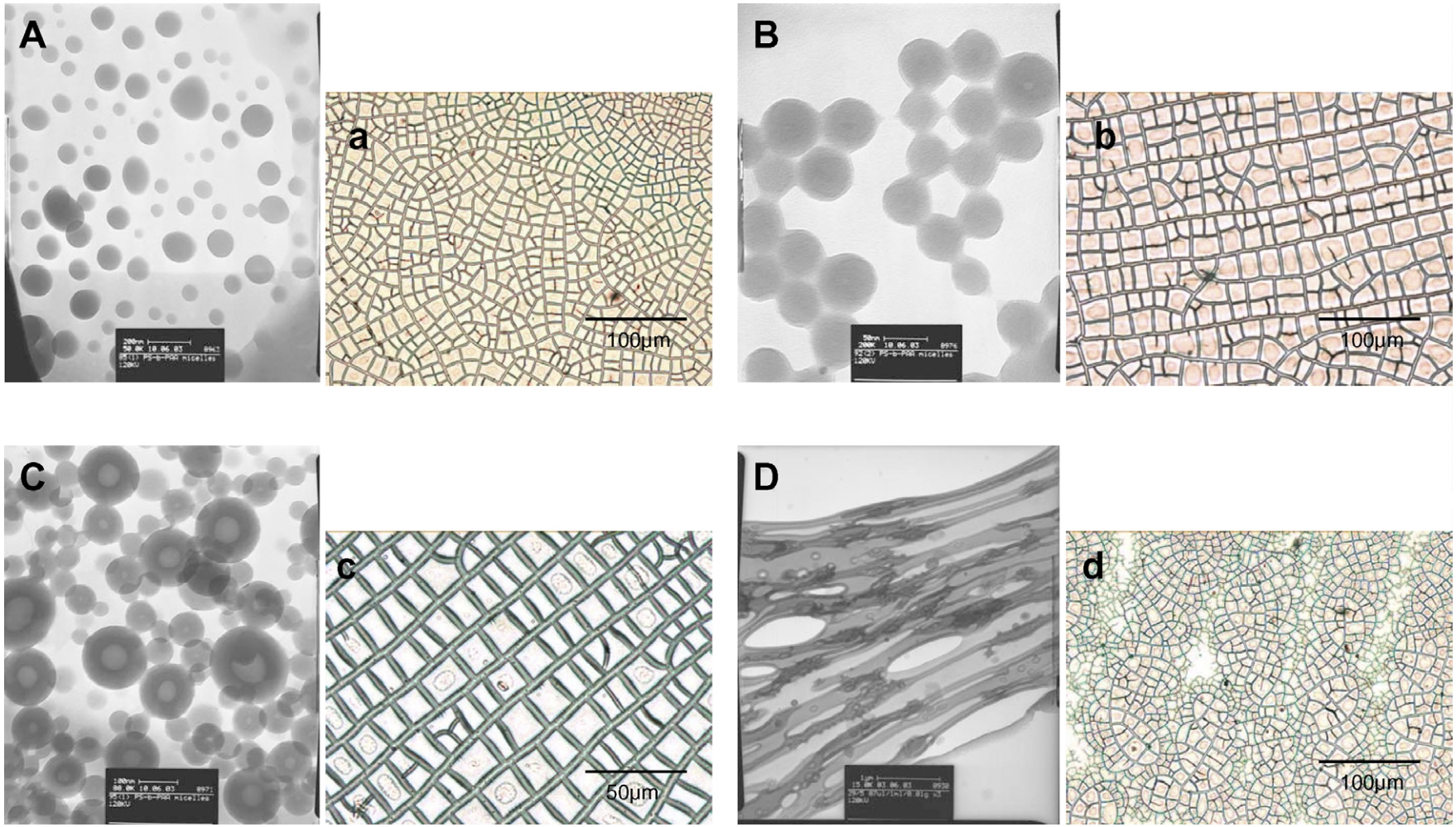

Fig. 5. Effect of micelle morphology on micropatterns. The transition of micelle morphology from spherical, to vesicular, and then to a mixture of cylindrical and lamella micelles by a progressive increase in water content from 0.080 v/v (A), 0.090 v/v (B), 0.095 v/v (C) to 0.10 v/v (D), and the corresponding evaporation-induced micropatterns (a–d).

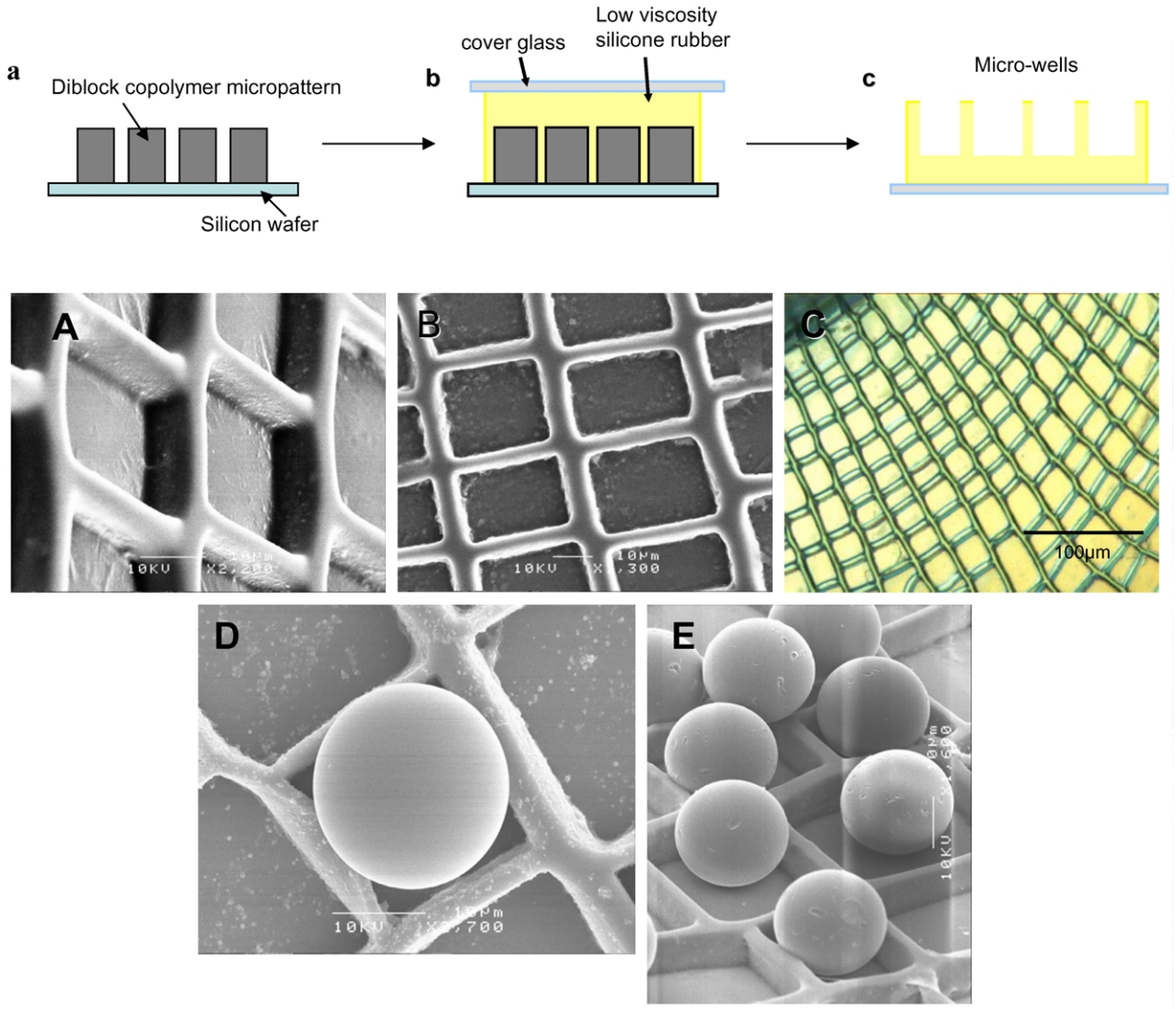

Fig. 6. Micromolding of silicone rubber microwells using diblock copolymer micropattern as template (a–c). The SEM micrographs (A, B) and optical micrographs (C) of silicone rubber microwells. The SEM micrographs of microparticles assembled into the silicone rubber microwells in a one-bead-one-well fashion (D, E).

orientating effect and, as a result, a highly ordered crack patterns can be formed [8,10]. For an evaporation system with a thinner layer and weaker drying front, the humidity change will be less abrupt and the cracks will propagate in a milder and less directional manner. This leads to the formation of wavy or branched crack patterns, and results in irregular and polygonal patterns of smaller sizes [6,8,10].

3.4. Effect of micelle morphology

As mentioned before, a number of colloidal systems have been previously used as experimental models for the study of crack formation. For all the experiments, uniformity and stability of the colloidal particles was an essential prerequisite. In our experiment, we investigated the potential impact of the variation of micelle morphology on the formation of crack pattern. We first used the amphiphillic diblock copolymer to prepare micelles with different sizes and structures in the aqueous solution. TEM micrographs of micelles with various morphologies were presented in Fig. 5(A)–(D). The corresponding crack patterns formed from different micelle morphologies at the same evaporation condition are demonstrated in Fig. 5(a)–(d). The morphology of diblock copolymer micelles shows a transition when the solvent content varies [15,16]. As illustrated in Fig. 5(A), micelles at the water content of 0.08 v/v were initially spherical in shape. Upon drying, mesh-like crack patterns were observed as shown in Fig. 5(a). By increasing the water content to 0.09 and 0.095 v/v, the micelles morphology transformed from spherical to vesicular, as reflected in Fig. 5(B) and (C), and a progressive improvement in the crack pattern regularity is seen in Fig. 5(b) and (c). A further increase in the water content to 0.1 v/v resulted in the mixed morphology of the micelles of

vesicular, tubular and lamella as illustrated in Fig. 5(D). A deterioration of pattern regularity was finally observed in Fig. 5(d). It can be concluded that crack patterns with high regularity were more likely to be developed from globular micelles. Therefore, the micelle morphology can be used as an indicator of the orderliness of the crack patterns induced by evaporation.

4. Conclusion and significance

We have demonstrated the feasibility of using diblock copolymer micelles as nano-building blocks to fabricate highly regular and orderly aligned three-dimensional micropatterns through a one-step evaporation-induced cracking process. A number of crack patterns in micron scale, including square, rectangular, stripe-like and mesh-like, structures were obtained. The effect of the concentration of the diblock copolymer, the substrates, the film thickness and the micelle morphologies on the regularity of crack patterns was studied. The evaporation-induced cracking provides a cheap, fast, simple and versatile means of microfabrication for patterned structures in micron scale. The crack patterns can be used as templates for molding polymer microwells. Fig. 6 shows the microwells of silicone rubber that was molded from one of the micropatterns of Fig. 1(D). The microwells can be potentially applied as high-density micro titer plates with nearly a million of sampling wells for analytical purpose. Fig. 6(D) and (E) further demonstrates that the polystyrene microparticles can be self-organized into the microwells and applied as bead-based biosensors or chip-based microarrays. Microparticles can be coated with biorecognition molecules like DNA-probes or antibodies as the sensing elements. The resulting bead-based DNA microarray or antibodies biosensors can be utilized in detecting the corresponding DNA samples and antigens. Micropatterns could also be used as templates for micromolding biodegradable or biocompatible materials into tissue culture scaffolds, which may play an important role in tissue engineering. Another potential application, in the microelectronic industries, is the microsilver meshwork fabricated by the templated silver reduction out of the diblock copolymer micropatterns. Silver microelectrodes could be fabricated with lower capital investment that will facilitate a broader development in the miniature electronic device industries and the microelectromechanical (MEM) technology.

Acknowledgements

The financial support of the RGC research grant, HKUST6195/01P, is gratefully acknowledged.

References

[1] Kitsunezaki S. Phys Rev E 1999;60:6449.
[2] Hull D, Caddock BD. J Mater Sci 1999;34:5707.
[3] Tompkins JQ. Geol Soc Am Bull 1965;76:1075.
[4] Muller G. J Geophys Res B 1998;103:15239.
[5] Lanchenbruch AH. Geol Soc Am Spec Pap 1962;70.
[6] Groisman A, Kaplan E. Europhys Lett 1994;25:415.
[7] Allain C, Limat L. Phys Rev Lett 1995;74:2981.
[8] Jagla EA. Phys Rev E 2002;65:046147.
[9] Pauchard L, Adda-Bedia M, Allain C, Couder Y. Phys Rev E 2003;67:027103.
[10] Shorlin KA, Bruyn JR, Graham M, Morris SW. Phys Rev E 2000;61(6):6950.
[11] (a) Zhang L, Eisenberg A. Science 1995;268:1728. (b) Zhang L, Eisenberg A. Macromolecules 1996;29:8805.
[12] Yu K, Eisenberg A. Macromolecules 1996;29:6359.
[13] Bronstein LM, Chernyshov DM, Timofeeva GI, Dubrovina LV, Valetsky PM. Langmuir 1999;15:6195.
[14] Cameron NS, Corbierre MK, Eisenberg A. Can J Chem 1995;77:1311.
[15] (a) Shen H, Eisenberg A. J Phys Chem B 1999;103:9473. (b) Shen H, Zhang L, Eisenberg A. J Am Chem Soc 1999;121:2728.
[16] (a) Burke SE, Eisenberg A. Langmuir 2001;17:6705. (b) Burke SE, Eisenberg A. Langmuir 2001;17:8341.